Spatiotemporal Dynamics of El Niño Modoki Impacts on East Java Rainfall Using EOF, BIRCH Clustering, and Wavelet Coherence

Diah Ariefianty[1], Agung Budi Susanto[2], Arya Adhyaksa Waskita[3]
[1,2,3] Master of Informatics Engineering Program, Universitas Pamulang, Kota Tangerang Selatan, Banten

Article Info

Article history:

Received Jul 04, 2026
Revised Jul 11, 2026
Accepted Nov 1, 2026

Corresponding Author:

Diah Ariefianty
Master of Informatics Engineering Program,
Universitas Pamulang, Kota Tangerang Selatan, Banten
Email:
vivieandrian@gmail.com

ABSTRACT

El Niño Modoki is a variation of El Niño characterized by sea-surface-temperature warming in the central Pacific, flanked by cooling in the eastern and western Pacific, and can influence rainfall patterns in Indonesia, particularly in East Java. This region was selected because it is one of Indonesia’s major food-producing areas, has high rainfall variability, and remains highly vulnerable to drought. This study aimed to analyze the impact of El Niño Modoki on monthly rainfall anomalies in East Java during 1991–2024. The data consisted of the El Niño Modoki Index (EMI) and monthly gridded rainfall data. The analytical methods included rainfall-anomaly calculation, Pearson correlation, Empirical Orthogonal Function (EOF), BIRCH clustering, Wavelet Coherence (WTC), and composite analysis. BIRCH clustering based on the first three EOF modes formed four rainfall-pattern clusters in East Java. WTC analysis showed that the relationship between EMI and rainfall was more dominant at interannual periods of approximately 1–4 years. Composite analysis indicated that El Niño Modoki reduced rainfall in East Java starting from the JJA period and became stronger and more spatially extensive during ASO. Overall, the impact of El Niño Modoki on East Java rainfall was spatial, seasonal, dynamic, and non-homogeneous across regions. These findings provide preliminary information for drought mitigation, water-resource management, and climate early-warning strengthening in East Java.

Keywords: BIRCH clustering,El Niño Modoki, Empirical Orthogonal Function, Wavelet Coherence

1. INTRODUCTION

Indonesia lies within the tropical maritime region, where rainfall variability emerges from interactions among monsoon circulation, sea–air coupling, complex topography, and large-scale climate modes (Mulsandi et al., 2024). El Niño–Southern Oscillation (ENSO) is one of the principal sources of interannual rainfall variability, but ENSO events are not spatially uniform and their characteristics have changed over recent decades (Wu et al., 2025). In addition to the conventional eastern-Pacific El Niño, central-Pacific warming can produce a distinct configuration commonly referred to as El Niño Modoki. This event is marked by positive sea-surface-temperature anomalies in the central tropical Pacific flanked by relatively cooler anomalies to the east and west, creating a tripolar pattern with teleconnections that differ from those of conventional El Niño (Ashok et al., 2007; Weng et al., 2007).

The distinction is important for Indonesia because the centers of convection and subsidence associated with the two El Niño types are displaced. Previous studies found that El Niño Modoki can suppress Indonesian rainfall, although its amplitude and spatial extent are generally weaker and less uniform than those associated with conventional El Niño (Iskandar et al., 2019). Windari et al. (2012) further showed that the influence of Modoki on monsoonal rainfall is particularly evident from the dry season into the transition season. Recent analysis of the Indonesian Maritime Continent also confirmed that El Niño-related rainfall anomalies differ markedly between southern and northern sectors (Zehri et al., 2025). These findings indicate that a national rainfall average can conceal substantial regional contrasts and that Modoki should be assessed at scales relevant to water and agricultural management.

El Niño Modoki is commonly quantified with the El Niño Modoki Index, which contrasts sea-surface-temperature anomalies in the central tropical Pacific with anomalies in the eastern and western Pacific. In conceptual form, EMI = SSTA_C − 0.5(SSTA_E) − 0.5(SSTA_W), where the central box covers approximately 165°E–140°W and 10°S–10°N, the eastern box covers 110°W–70°W and 15°S–5°N, and the western box covers 125°E–145°E and 10°S–20°N. A positive EMI therefore represents central-Pacific warming accompanied by relative cooling on both sides of the basin.

The physical importance of this configuration lies in the displacement of deep convection and the associated Walker-circulation anomalies. Conventional El Niño shifts the principal warming and atmospheric response farther east, whereas Modoki retains the strongest warming closer to the central Pacific. The resulting circulation can reduce moisture convergence over parts of the Maritime Continent while producing a teleconnection footprint that differs from event to event. Figure 1 summarizes the conceptual contrast among conventional El Niño structures and the Modoki configuration.

East Java rainfall is particularly sensitive to this circulation because the province sits on the southern side of the Maritime Continent and is strongly monsoonal. During the dry season, background subsidence and southeasterly flow already limit moisture availability. An additional central-Pacific forcing can therefore amplify rainfall deficits or delay the seasonal transition, but the response is modified by mountains, coastlines, and local sea–land contrasts. This physical setting motivated a regional rather than national analysis.

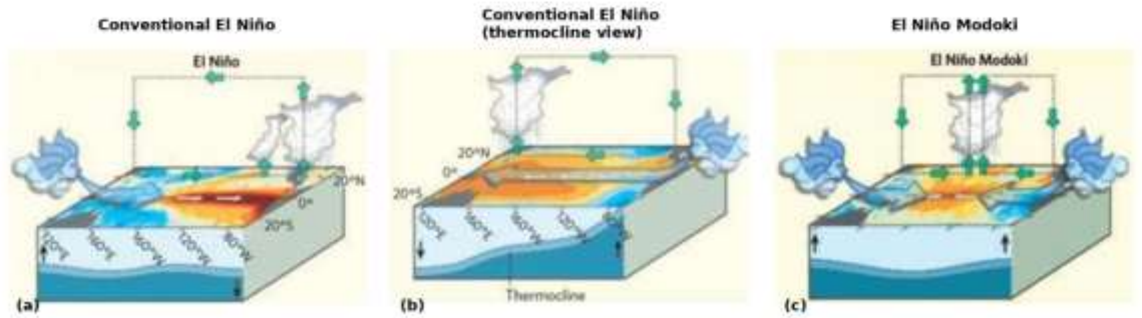

Figure 1. Conceptual comparison of conventional El Niño configurations and El Niño Modoki, emphasizing the displacement of the warm pool and thermocline response

East Java provides a strategically important regional case. The province includes low-lying northern coastal areas, Madura Island, volcanic highlands, southern mountain ranges, and eastern peninsular environments. These geographic contrasts interact with monsoon flow and local land–sea processes to produce pronounced spatial rainfall differences. Rainfall periodicity in East Java has been associated with ENSO, the Indian Ocean Dipole, the Madden–Julian Oscillation, monsoon indices, and topographic setting (Bimaprawira & Rejeki, 2021). The province is also a major food-production region, while agricultural vulnerability to drought is uneven and particularly pronounced in parts of Madura and northern East Java (Mulyanti et al., 2023). A long and internally consistent rainfall record is therefore essential for identifying areas and seasons in which Modoki-related rainfall deficits may pose the greatest risk (Mulyanti et al., 2024).

A single correlation coefficient is insufficient to describe this problem. Rainfall fields contain coherent regional signals, local contrasts, and non-stationary relationships with large-scale climate indices. Empirical Orthogonal Function (EOF) analysis provides an objective means of reducing a high-dimensional rainfall field into dominant spatial modes and corresponding temporal principal components. Indonesian studies demonstrated that a small number of EOF modes can represent major monsoonal, equatorial, and local rainfall structures at national and regional scales (Ariska et al., 2024a, 2024b, 2024c; Sayyendra et al., 2025). However, EOF loadings are continuous and do not directly define operationally interpretable rainfall zones.

To translate the EOF patterns into regional groupings, this study applied Balanced Iterative Reducing and Clustering Using Hierarchies (BIRCH). BIRCH summarizes large numerical datasets through clustering features and a compact tree structure, allowing efficient grouping without repeatedly processing all observations (Zhang et al., 1996). Later developments showed that dynamic thresholds and improved clustering-feature trees can strengthen cluster quality, efficiency, and numerical stability (Ramadhani et al., 2020; Lang & Schubert, 2022). Its use after EOF enables grid cells with similar combinations of dominant rainfall modes to be grouped as climatological zones rather than administrative units.

The temporal relationship between a climate index and rainfall may also strengthen or weaken at different periods. Wavelet Coherence (WTC) addresses this limitation by resolving local association in both time and frequency. Wavelet applications to rainfall have demonstrated their usefulness for identifying non-stationary temporal structures (Ruwangika et al., 2020), while ENSO–precipitation studies have revealed intermittent interannual bands, phase opposition, and possible lead–lag behavior that are hidden by full-period correlation (Díaz & Villegas, 2022; Hussain et al., 2022). Seasonal composite analysis complements these methods by showing the spatial rainfall difference between Modoki and neutral years.

Despite the relevance of these approaches, limited work has integrated gridwise correlation, EOF, BIRCH clustering, WTC, and seasonal composites to examine El Niño Modoki specifically in East Java. This study therefore addressed four questions: how EMI was related to rainfall anomalies across East Java; which dominant rainfall modes and regional clusters characterized the province; when and at what periods the EMI–rainfall relationship became coherent; and how rainfall during Modoki years differed from neutral conditions in June–August (JJA) and August–October (ASO). The main contribution is an integrated spatial, regional, and time–frequency framework that converts long-term climate data into information applicable to drought preparedness, cropping-calendar adjustment, and climate early-warning services.

Based on the identified research gap, this study aims to analyze the impact of El Niño Modoki on monthly rainfall anomalies in East Java during 1991–2024 by integrating Pearson correlation, Empirical Orthogonal Function, BIRCH clustering, Wavelet Coherence, and composite analysis. The study focuses on identifying the relationship between EMI and rainfall anomalies, extracting dominant spatiotemporal rainfall patterns, grouping regions with similar rainfall characteristics, examining the time–frequency dynamics of the EMI–rainfall relationship, and evaluating rainfall changes during El Niño Modoki events compared with neutral years. The results are expected to provide a more comprehensive understanding of Modoki-related rainfall variability in East Java and to support drought mitigation, water-resource management, agricultural planning, and climate early-warning services.

2. PREVIOUS STUDIES AND RESEARCH GAP

Earlier studies established the relevance of Modoki for Indonesian rainfall, but most were conducted at national scale or relied on a single analytical perspective. Composite studies demonstrated broad drying, national EOF studies identified dominant rainfall structures, and WTC studies in other regions revealed intermittent teleconnections. Few studies combined these perspectives at provincial scale, and the use of BIRCH after EOF to create climate-response zones remains uncommon in Indonesian rainfall research.

Table 1. Position of the study relative to selected previous research

Study	Area and Method	Remaining gap addressed here
Windari et al. (2012)	Indonesian monsoonal regions; correlation, wavelet, and composites	No province-specific EOF regionalization for East Java
Iskandar et al. (2019)	Indonesia; seasonal composites of conventional and Modoki El Niño	Limited local spatial detail and no time–frequency cluster analysis
Ariska et al. (2024a, 2024b, 2024c)	Indonesia; EOF, correlation, FFT, and composites	National-scale modes may mask East Java subregional contrasts
Díaz and Villegas (2022)	Colombian Andes; WTC of ENSO and precipitation	Different climate region and no EOF-based rainfall zones
Present study	East Java; correlation, EOF, BIRCH, WTC, and composites	Integrated regional and time–frequency assessment

The novelty of the present work is therefore methodological and regional. It links the physical Modoki index to a gridwise rainfall response, extracts dominant spatial modes, converts those modes into four interpretable rainfall zones, evaluates cluster-specific time–frequency coherence, and tests seasonal impact through composites. This sequence provides a more complete account of where, when, and during which seasonal window Modoki-related drying becomes relevant in East Java.

3. RESULT AND ANALYSIS

3.1. DATASET

The study covered East Java Province and used monthly data from January 1991 through December 2024. El Niño Modoki variability was represented by the monthly El Niño Modoki Index (EMI) obtained from the Interactive Tool for Analysis of the Climate System of the Japan Meteorological Agency. Rainfall was represented by a gridded monthly dataset supplied by the Indonesian Agency for Meteorology, Climatology, and Geophysics. The datasets were synchronized to a common monthly time axis, producing 408 observations for each retained rainfall grid.

Initial quality control checked temporal completeness, duplicate timestamps, variable units, and spatial coverage. Only rainfall grids located within East Java and containing an adequate monthly record were retained. EMI was treated as the explanatory climate index, while rainfall anomaly at each grid was the response variable. The analysis was conducted in Python on Google Colab using numerical, machine-learning, wavelet, and geospatial libraries.

Table 2. Data sources and analytical framework

Variable	Unit	Description
EMI	Monthly ITACS–JMA index, 1991–2024	Climate forcing and Modoki-event identification
Rainfall	Monthly BMKG gridded rainfall over East Java	Anomaly, EOF, clustering, WTC, and composites
Temporal scale	408 monthly observations	Long-term and interannual analysis
Seasonal windows	JJA and ASO	Dry-season and late-dry/transition composites
Software	Python in Google Colab	Data processing, statistics, clustering, and mapping

The complete analytical sequence is summarized in Figure 1. The workflow was designed so that each method answered a different part of the research problem. Correlation described the average linear relationship at each grid; EOF extracted dominant spatial structures; BIRCH translated those structures into regional rainfall zones; WTC identified when and at which periods EMI and rainfall became coherent; and composites quantified the seasonal spatial response during Modoki events. Using these methods together reduced the risk of drawing conclusions from a single statistic.

3.2. FLOWCHART

The research was conducted through a sequence of climate-data analysis stages. The first stage involved collecting monthly EMI data and monthly gridded rainfall data for East Java from 1991 to 2024. The second stage consisted of checking data completeness, format consistency, temporal alignment, and spatial coverage. The third stage calculated monthly rainfall anomalies by subtracting the long-term climatological mean of the corresponding calendar month from the observed rainfall value. The fourth stage identified El Niño Modoki years based on sustained positive EMI phases and supporting classifications from previous studies. The fifth stage examined the relationship between EMI and rainfall anomalies using gridwise Pearson correlation. The sixth stage applied EOF analysis to extract dominant spatiotemporal rainfall-variability modes. The seventh stage used BIRCH clustering to group rainfall grids according to similarities in the selected EOF loadings. The eighth stage applied Wavelet Coherence to analyze the time–frequency dynamics between EMI and cluster-mean rainfall anomalies. The ninth stage used composite analysis to compare rainfall conditions during El Niño Modoki years and neutral years for JJA and ASO. The final stage integrated all analytical outputs to interpret the spatial, seasonal, and temporal characteristics of El Niño Modoki impacts on East Java rainfall.

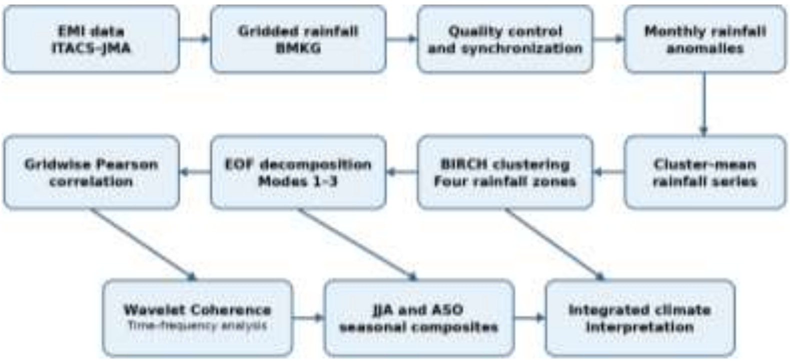

Figure 2. Integrated analytical workflow for assessing El Niño Modoki impacts on East Java rainfall

3.3. RAINFALL ANOMALY AND SPATIAL CORRELATION

For each grid, the climatological mean of each calendar month was computed from the 1991–2024 record. Monthly rainfall anomalies were then calculated as the departure of an observed monthly value from the corresponding calendar-month climatology:

$$A_{i,j,t} = R_{i,j,t} - R_{i,j,m} \qquad (1)$$

where $A_{i,j,t}$ is the anomaly at grid (i,j) and time t, $R_{i,j,t}$ is observed rainfall, and $R_{i,j,m}$ is the long-term mean for calendar month m. Gridwise Pearson correlations were calculated between EMI and rainfall anomalies. Negative coefficients indicated that positive EMI conditions tended to coincide with lower-than-normal rainfall. Correlation values were interpolated with inverse distance weighting for continuous visualization, while interpretation remained anchored to the original grids

3.4. EOF AND BIRCH CLUSTERING

The rainfall-anomaly field was arranged as a time-by-space matrix. After centering, EOF decomposition represented the field as a linear combination of orthogonal spatial loadings and temporal principal components:

$$X(s,t) = \Sigma\, PC_k(t)\, EOF_k(s) \qquad (2)$$

The leading modes were selected according to explained variance and climatological interpretability. The first three loading values at each grid were standardized and used as BIRCH features. Candidate thresholds were evaluated to balance cluster stability, spatial coherence, and the preservation of regional detail. A threshold of 1.8 produced four interpretable clusters and was retained, even though a coarser three-cluster solution at a higher threshold yielded a somewhat larger silhouette value. This choice avoided excessive simplification of local rainfall contrasts. The final clusters were mapped and their monthly rainfall climatologies were compared.

3.5. WAVELET COHERENCE AND COMPOSITE ANALYSIS

Wavelet Coherence was applied to examine the local relationship between EMI and rainfall anomalies in both time and frequency domains. This method was used because the relationship between climate indices and rainfall is not always stationary throughout the observation period. For each BIRCH cluster, rainfall anomalies were spatially averaged to form a monthly cluster series. The WTC analysis was then performed between EMI and each cluster-mean rainfall anomaly series to identify when the relationship strengthened, at which dominant periods it occurred, and whether the phase relationship indicated an inverse association between EMI and rainfall.

Wavelet Coherence (WTC) was applied to examine the local relationship between EMI and rainfall anomalies in both time and frequency domains. For each BIRCH cluster, rainfall anomalies were spatially averaged to form a monthly cluster series. In this study, the continuous wavelet transform was performed using the Morlet mother wavelet, which provides an optimal balance between time and frequency localization for geophysical time series. The statistical significance of the coherence was strictly assessed against a red noise (first-order autoregressive, AR1) background spectrum. To establish the significance threshold, a Monte Carlo simulation with 1,000 iterations was conducted, configuring the significance test at a 95% confidence level ($\alpha = 0.05$). In the resulting visualization, coherence values range from zero to one. Regions enclosed by thick black contours denote statistically significant associations at the 95% confidence level. Interpretation predominantly focused on these significant regions located outside the cone of influence (COI) to avoid edge effects.

Modoki and neutral years were identified from sustained positive EMI phases and supporting event classifications in the literature. Seasonal composite rainfall was calculated as the mean rainfall during Modoki years minus the corresponding mean during neutral years. The analysis was performed for JJA and ASO. Negative composite values indicated rainfall deficits during Modoki conditions. The composites were compared with EOF1 reconstructions and BIRCH boundaries to evaluate the consistency of spatial signals across methods.

3.6. EVALUATION AND INTERPRETATION CRITERIA

The analysis did not construct a forecasting model; consequently, evaluation was based on statistical consistency, spatial representativeness, and agreement across methods rather than predictive error metrics. Pearson coefficients were interpreted by direction, magnitude, and spatial continuity. EOF modes were evaluated through explained variance, spatial coherence, and the climatic plausibility of their principal-component behavior. The cumulative variance of the retained modes was reported to make the dimensional reduction explicit.

BIRCH solutions were compared across candidate thresholds. Silhouette Score, Davies–Bouldin Index, and Calinski–Harabasz Index were considered where available, but the final decision also accounted for the stability of the number of clusters, geographic coherence, and retention of the north–south and west–east contrasts identified by EOF. This mixed evaluation was necessary because a numerically compact solution can merge regions that are climatically distinct.

WTC interpretation emphasized coherence enclosed by the 95% significance contour and located outside the cone of influence. Areas near the beginning and end of the record were treated cautiously because padding and finite-series effects can inflate apparent coherence. Phase arrows were interpreted as indicators of relative timing, not as definitive proof of causality. Seasonal composites were evaluated for sign, spatial extent, contrast between JJA and ASO, and consistency with the correlation and EOF results.

Robustness was assessed through convergence among methods. A Modoki-related drying signal was considered more credible when it appeared as negative gridwise correlation, negative seasonal composite rainfall, a coherent EOF1 reconstruction, and inverse WTC phase behavior during significant intervals. This triangulation provided a stronger basis for interpretation than any individual analysis alone.

4. RESULT AND ANALYSIS

4.1. RESEARCH DATA CHARACTERISTICS

The analysis began by calculating monthly rainfall anomalies to identify deviations from the climatological condition of East Java rainfall. Rainfall anomalies were obtained by subtracting the long-term mean rainfall of the corresponding calendar month from the observed monthly rainfall value at each grid. Positive anomalies indicate wetter-than-normal conditions, whereas negative anomalies indicate drier-than-normal conditions. The gridded rainfall data were then spatially averaged to provide a regional overview and visually compared with the EMI time series from January 1991 to December 2024.

The regional mean rainfall anomaly fluctuated substantially during the study period, indicating that East Java experienced alternating wet and dry episodes rather than a stable long-term rainfall condition.

Pronounced negative anomalies appeared around 1997–1998, 2002–2004, 2006, 2015, 2019, and 2023, while positive anomalies were observed around 1992, 1998–1999, 2010, 2013, 2016, 2020–2022, and 2024. Several positive EMI phases coincided with negative rainfall anomalies, suggesting that increasing EMI was associated with rainfall reduction in East Java during certain periods. However, the relationship was not consistent throughout the full record, indicating that EMI alone did not control all wet and dry episodes in the region.

The spatial correlation analysis in Figure 3(b) produced predominantly negative coefficients ranging from approximately −0.09 to −0.24. More negative values appeared in parts of southern and eastern East Java, while many central and northern areas remained closer to zero. The overall direction was consistent with the expected suppression of rainfall during positive EMI conditions, but the magnitude indicated a weak linear relationship. This result agrees with findings that Modoki affects Indonesian rainfall less uniformly than conventional El Niño (Iskandar et al., 2019). It also reflects the influence of monsoon circulation, local sea-surface temperature, the Indian Ocean Dipole, intraseasonal convection, and terrain, none of which were represented directly by EMI.

The weak full-period correlation should not be interpreted as evidence that Modoki was unimportant. A correlation coefficient averages across months and years, including intervals when the teleconnection was weak or absent. The later WTC results showed that the relationship became much stronger during selected interannual intervals. Thus, Pearson correlation served as a spatial screening tool, while EOF, clustering, WTC, and composites were required to characterize the structure and timing of the response.

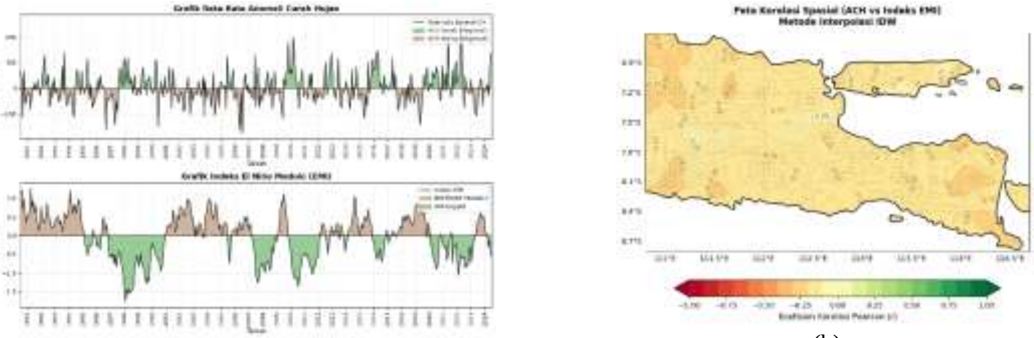

(a) (b)

Figure 3. (a) East Java regional mean rainfall anomaly and EMI time series, 1991–2024; (b) spatial Pearson correlation between EMI and rainfall anomaly. Compiled from Thesis Figures 4.1 and 4.2

4.2. DOMINANT EOF MODES

The first three EOF modes jointly explained 52.4% of total rainfall-anomaly variance. EOF1 alone accounted for 43.8%, indicating that a broad regional signal dominated the monthly anomaly field. Its loadings had a largely common sign over the province, implying that large portions of East Java frequently became wetter or drier together. This coherent mode is compatible with province-wide forcing by monsoon variability and large-scale ocean–atmosphere anomalies.

EOF2 explained 4.4% and introduced a north–south contrast. Northern coastal and parts of Madura tended to have loadings of one sign, while southern mountain and coastal areas tended to have the opposite sign. EOF3 explained 4.2% and emphasized a west–east contrast, particularly distinguishing the eastern peninsula and Tapal Kuda region from western and central East Java. Although EOF2 and EOF3 explained much less variance than EOF1, their spatial contrasts were essential because they represented local departures from the regional mean response.

Table 3. Variance contribution and interpretation of the leading EOF modes

Mode	Explained variance	Dominant spatial interpretation
EOF1	43.8%	Coherent province-wide rainfall-anomaly variability
EOF2	4.4%	North–south contrast, including coastal and southern highland differences

Mode	Explained variance	Dominant spatial interpretation
EOF3	4.2%	West–east contrast, highlighting eastern East Java
Cumulative	52.4%	Regional signal plus two principal local contrasts

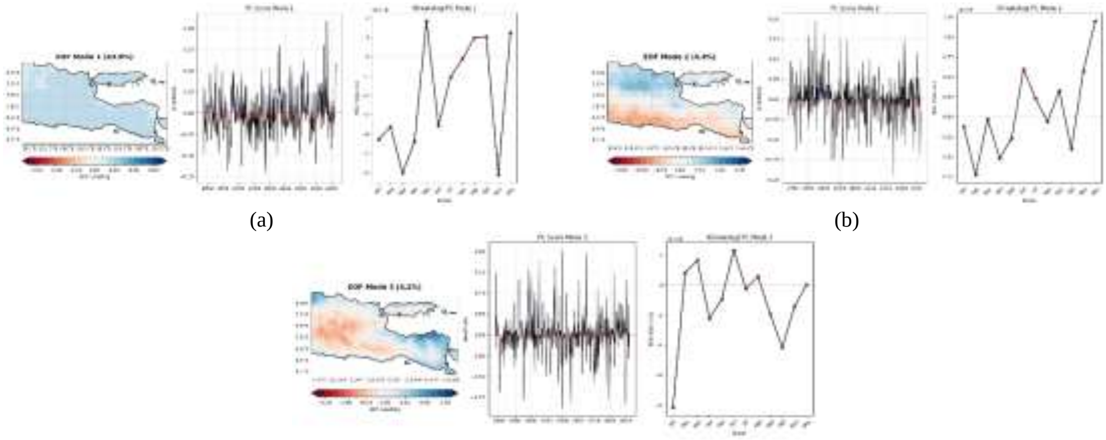

(a) (b)

(c)

Figure 4. Spatial loadings, temporal principal-component scores, and monthly PC climatologies for (a) EOF1, (b) EOF2, and (c) EOF3

The dominance of EOF1 is comparable with Indonesian EOF studies in which the leading mode represents broad monsoonal variability, while subsequent modes reveal equatorial or localized structures (Ariska et al., 2024a, 2024b). However, the East Java modes should not be assigned directly to national rainfall regimes. Their value lies in identifying province-specific contrasts shaped by the Java Sea, the Indian Ocean, volcanic topography, and the eastward narrowing of the island. The three modes therefore provided an appropriate low-dimensional feature set for clustering.

4.3. REGINALIZATION WITH BIRCH

BIRCH clustering of the standardized EOF1–EOF3 loadings produced four spatially coherent rainfall-pattern zones (Figure 5). The clusters did not follow administrative boundaries because they represented climatological similarity at grid scale. Consequently, a district could intersect more than one cluster when its terrain and rainfall regime varied internally. This is an advantage for climate analysis because atmospheric and topographic transitions rarely coincide exactly with political borders.

Table 4. General characteristics of the four BIRCH rainfall-pattern clusters

Cluster	General spatial character	Rainfall climatology and sensitivity
1	Southern and southeastern highland/coastal sectors	Relatively wet in the rainy season; strong topographic modulation
2	Central-to-eastern transition and selected coastal areas	Sharper dry-season decline, particularly in July–September
3	Western–central upland and southwestern sectors	Relatively high wet-season rainfall and strong local variability
4	Northern lowlands, Pantura, Surabaya surroundings, and parts of Madura	Lower wet-season intensity and generally drier background conditions

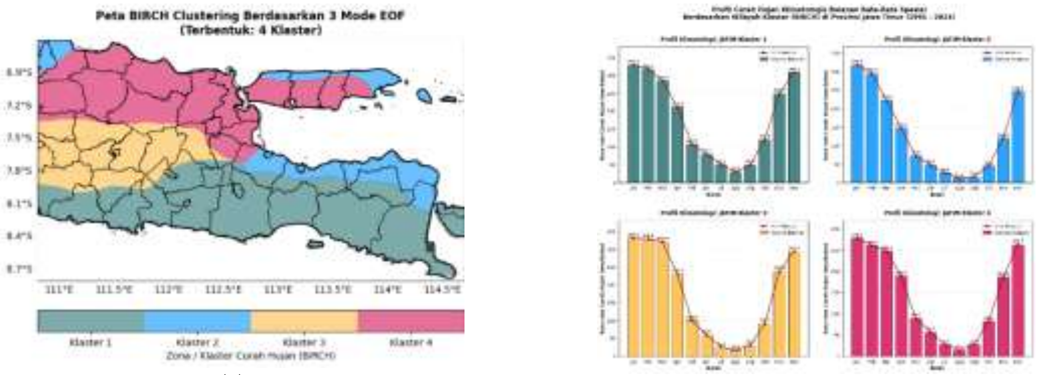

(a) (b)

Figure 5. (a) . Four East Java rainfall-pattern clusters derived from BIRCH applied to the first three EOF loading fields ; (b) Monthly rainfall climatology of the four BIRCH clusters, showing a common monsoonal cycle with different rainfall amplitudes

The BIRCH clustering results formed four main rainfall-pattern clusters that represented different rainfall characteristics across East Java. Cluster 1 was mainly associated with southern, central, and parts of eastern East Java, including areas with complex topography such as mountains, hills, and southern coastal zones. Cluster 2 included parts of Madura, the northern coast, and eastern East Java, representing a transition zone between northern, Madurese, and eastern rainfall characteristics. Cluster 3 was mostly associated with western, southwestern, and central East Java, reflecting rainfall variability influenced by inland topography and upland terrain. Cluster 4 was dominated by northern East Java, the Pantura region, Surabaya–Sidoarjo, and parts of Madura, which are generally characterized by lowland and northern coastal environments facing the Java Sea.

These clusters should be interpreted as climatological rainfall-pattern zones rather than strict administrative boundaries. One district or city may appear in more than one cluster because the clustering was performed at the grid level using EOF loading similarities, not based on administrative borders. Therefore, the BIRCH result helps explain why rainfall responses to El Niño Modoki are not homogeneous across East Java.

All four clusters retained a monsoonal annual cycle, with rainfall maxima generally occurring from November to March and minima from July to September. Their amplitudes differed, however. Clusters 1 and 3 were wetter during the rainy season, Cluster 2 exhibited a more abrupt dry-season reduction, and Cluster 4 had lower rainfall intensity overall. The result supported the interpretation of BIRCH as a regionalization tool: it preserved the shared monsoonal cycle while separating zones according to the strength and spatial expression of that cycle.

The selected threshold of 1.8 represented a compromise between internal validity metrics and climatic interpretability. A higher threshold merged spatially distinct areas into only three groups, obscuring differences that were visible in EOF2 and EOF3. Cluster evaluation in climate studies should therefore not rely exclusively on a single numerical index. Spatial contiguity, topographic plausibility, seasonal profiles, and usefulness for downstream analysis are also important. The four-cluster solution was retained because it provided a more informative basis for cluster-specific WTC analysis and adaptation planning.

4.4. TIME-FREQUENCY RELATIONSHIP BETWEEN EMI AND CLUSTER RAINFALL

Wavelet Coherence revealed that the relationship between EMI and rainfall anomalies was non-stationary in all four clusters. The relationship did not remain constant throughout 1991–2024, but strengthened only during certain periods and at specific time scales. In Cluster 1, relatively strong coherence appeared mainly at interannual periods of approximately 1–4 years, with significant areas emerging around the mid-1990s, early 2000s, and around 2015. This pattern indicates that the EMI–rainfall relationship in Cluster 1 was prominent at interannual scales, although it did not persist continuously throughout the entire record.

Clusters 2, 3, and 4 showed broadly similar behavior, with coherence appearing intermittently at periods of about 1–2 years and, in some cases, broader 4–7-year bands. The statistical significance of these patches was robustly confirmed by the Monte Carlo-generated 95% confidence contours. However, several high-coherence areas at longer periods were located near or within the cone of influence, and therefore must be interpreted cautiously because they may be affected by edge effects. The most reliable interpretation is that El Niño Modoki influence on East Java rainfall was most clearly expressed at interannual periods, particularly around 1–4 years.

Phase arrows in several significant areas indicated an inverse relationship, meaning that positive EMI variations were associated with negative rainfall anomalies. This result explains why the Pearson correlation was weak when calculated over the entire record: the EMI–rainfall relationship was not continuously active, but emerged episodically at certain times and periods. Therefore, WTC provided a more detailed explanation of the dynamic and time-varying nature of Modoki-related rainfall variability than a single linear correlation coefficient.. Coherence strengthened intermittently rather than remaining high throughout the 34-year record. The most recurrent significant structures occurred at approximately 1–4-year periods, consistent with interannual ENSO-type variability. Cluster 1 displayed relatively broad coherence during parts of the mid-1990s, early 2000s, and around 2015. Clusters 2–4 showed similarly intermittent patches, with prominent signals near 1–2 years and some broader 2–4-year intervals.

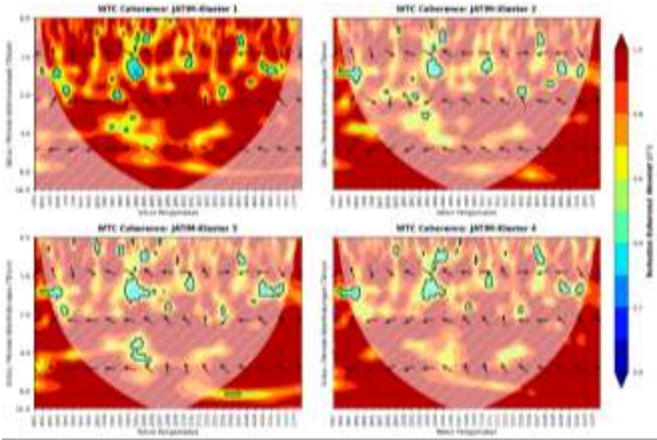

Figure 6. Wavelet Coherence between EMI and cluster-mean rainfall anomalies using the Morlet mother wavelet. Thick black contours denote statistically significant coherence at the 95% confidence level based on 1,000 Monte Carlo simulations against a red noise background. Interpretation emphasized regions outside the cone of influence (white shaded area).

Phase arrows in several significant areas indicated an inverse relationship, meaning that positive EMI variations were associated with negative rainfall anomalies. The direction was not uniform across all times and clusters, suggesting that local rainfall could respond with different timing or be modified by concurrent climate drivers. Strong coherence at periods longer than four years was frequently near the cone of influence and was therefore interpreted cautiously. The most robust conclusion was that Modoki influence emerged episodically at interannual scales rather than as a constant province-wide control.

This finding reconciles the weak Pearson coefficients with the clear physical and composite signals. Pearson correlation compressed the complete record into one number and consequently diluted intervals of strong coupling with intervals of little association. WTC isolated those intervals and confirmed that different rainfall zones did not respond identically. Similar time-varying behavior has been reported for ENSO–precipitation relationships in other monsoon and tropical regions (Díaz & Villegas, 2022; Hussain et al., 2022).

4.5. SEASONAL COMPOSITE IMPACT OF EL NIÑO MODOKI

Composite analysis was conducted to examine the spatial impact of El Niño Modoki on rainfall in East Java by comparing rainfall during Modoki years with rainfall during neutral years. This analysis was performed for two seasonal periods: JJA, representing the dry season, and ASO, representing the late dry season to the transition toward the rainy season. Negative composite values indicate lower rainfall during El Niño Modoki years than during neutral years, whereas positive values indicate wetter conditions.

During JJA, most clusters showed reduced rainfall relative to neutral conditions. The reduction was spatially extensive, particularly across southern, central, and parts of eastern East Java. This pattern indicates that El Niño Modoki tends to strengthen dry-season rainfall deficits in the study area. However, some local areas showed near-normal or slightly positive values, confirming that the impact was not spatially uniform across the province.

During ASO, the rainfall deficit became stronger and more widespread than during JJA. The dominance of negative composite values indicates that reduced rainfall associated with El Niño Modoki can persist into the late dry season and the transition toward the rainy season. This suggests that El Niño Modoki may delay or weaken the early recovery of rainfall, especially during September and October. The EOF1 reconstruction showed a pattern consistent with the actual rainfall composite, indicating that the leading EOF mode successfully captured the dominant drying signal associated with El Niño Modoki events.

Overall, the composite results support the previous findings from Pearson correlation, EOF, BIRCH clustering, and WTC. Pearson correlation indicated a general negative tendency between EMI and rainfall anomalies, EOF identified dominant regional and local rainfall structures, BIRCH separated areas with different rainfall characteristics, and WTC showed that the EMI–rainfall relationship strengthened at certain periods. Composite analysis provided the most direct spatial evidence that El Niño Modoki was associated with rainfall reduction in East Java, beginning in JJA and becoming stronger and more extensive during ASO.

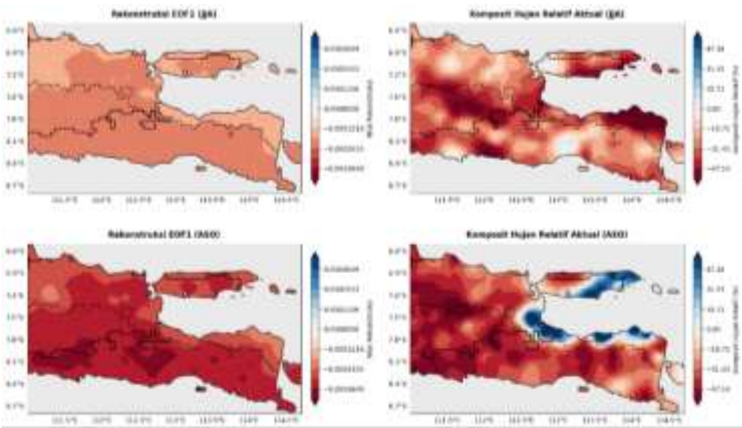

Figure 7. EOF1 reconstruction and relative rainfall composite during El Niño Modoki years for JJA and ASO

The composite, EOF, cluster, and WTC results were mutually supportive. Correlation indicated a province-wide tendency toward reduced rainfall as EMI increased. EOF1 identified a coherent regional anomaly, while EOF2 and EOF3 explained why the response departed from uniformity. BIRCH converted these contrasts into four rainfall zones. WTC showed that the relationship strengthened during selected interannual intervals, and composites demonstrated that the most widespread negative impacts occurred during the dry season and became stronger during ASO. The integrated evidence therefore supported a spatially heterogeneous, seasonally dependent, and temporally intermittent Modoki influence.

5. CONCLUTION

This study analyzed the impact of El Niño Modoki on East Java rainfall during 1991–2024 by integrating rainfall-anomaly calculation, Pearson correlation, Empirical Orthogonal Function, BIRCH clustering, Wavelet Coherence, and composite analysis. The results showed that EMI had a generally negative relationship with rainfall anomalies in East Java, indicating that increasing EMI tended to be associated with reduced rainfall. EOF analysis identified three dominant rainfall-variability patterns: EOF1 explained 43.8% of the variance and represented a relatively coherent regional mode, EOF2 explained 4.4% and captured a north–south contrast, while EOF3 explained 4.2% and represented a west–east contrast. BIRCH clustering based on the first three

EOF modes produced four rainfall-pattern clusters with different characteristics: Clusters 1 and 3 tended to have higher rainfall, Cluster 2 showed a sharper dry-season decline, and Cluster 4 experienced the driest dry-season condition, particularly across northern East Java and Madura. WTC analysis demonstrated that the EMI–rainfall relationship was non-stationary, with dominant coherence mainly at interannual periods of about 1–4 years and inverse phase behavior indicating that positive EMI was associated with negative rainfall anomalies. Composite analysis further confirmed that El Niño Modoki reduced rainfall in East Java starting in JJA and became stronger and more spatially extensive during ASO. Overall, the impact of El Niño Modoki on East Java rainfall was spatial, seasonal, dynamic, and non-homogeneous across regions. These results can serve as preliminary information for drought mitigation, water-resource management, agricultural planning, and the strengthening of climate early-warning systems in East Java.

ACKNOWLEDGEMENTS

The author gratefully acknowledges the Indonesian Agency for Meteorology, Climatology, and Geophysics for the gridded rainfall data, the Japan Meteorological Agency for the EMI data, and the Master of Informatics Engineering Program at Universitas Pamulang for academic support. The author also thanks the Climate Early Warning team for technical discussions during data preparation and interpretation.

REFERENCES

Ariska, M., Suhadi, S., Supari, S., Irfan, M., & Iskandar, I. (2024a). Annual and interannual rainfall variability in Indonesia using empirical orthogonal function analysis and its response to ocean–atmosphere dynamics. *Jurnal Ilmu Fisika, 16*(2), 151–165. https://doi.org/10.25077/jif.16.2.151-165.2024

Ariska, M., Suhadi, Supari, Irfan, M., & Iskandar, I. (2024b). Detection of dominant rainfall patterns in Indonesian regions using empirical orthogonal function and its relation with ENSO and IOD events. *Science and Technology Indonesia, 9*(4), 1009–1023. https://doi.org/10.26554/sti.2024.9.4.1009-1023

Ariska, M., Suhadi, Supari, Irfan, M., & Iskandar, I. (2024c). Spatio-temporal variations of Indonesian rainfall and their links to Indo-Pacific modes. *Atmosphere, 15*(9), Article 1036. https://doi.org/10.3390/atmos15091036

Ashok, K., Behera, S. K., Rao, S. A., Weng, H., & Yamagata, T. (2007). El Niño Modoki and its possible teleconnection. *Journal of Geophysical Research: Oceans, 112*(C11), 1–27. https://doi.org/10.1029/2006JC003798

Bimaprawira, A. K., & Rejeki, H. A. (2021). Keterkaitan periodisitas curah hujan di daerah pesisir dan pegunungan Provinsi Jawa Timur dengan variabilitas cuaca skala global dan regional. *Jurnal Sains & Teknologi Modifikasi Cuaca, 22*(2), 51–59.

Díaz, D., & Villegas, N. (2022). Wavelet coherence between ENSO indices and two precipitation databases for the Andes region of Colombia. *Atmósfera, 35*(2), 237–271. https://doi.org/10.20937/ATM.52890

Hussain, A., Cao, J., Ali, S., Ullah, W., Muhammad, S., Hussain, I., Abbas, H., Hamal, K., Sharma, S., Akhtar, M., Wu, X., & Zhou, J. (2022). Wavelet coherence of monsoon and large-scale climate variabilities with precipitation in Pakistan. *International Journal of Climatology*. https://doi.org/10.1002/joc.7874

Iskandar, I., Lestari, D. O., & Nur, M. (2019). Impact of El Niño and El Niño Modoki events on Indonesian rainfall. *Makara Journal of Science, 23*(4), 217–222. https://doi.org/10.7454/mss.v23i4.11517

Lang, A., & Schubert, E. (2022). BETULA: Fast clustering of large data with improved BIRCH CF-trees. *Information Systems, 108*, Article 101918. https://doi.org/10.1016/j.is.2021.101918

Mulsandi, A., Koesmaryono, Y., Hidayat, R., Faqih, A., & Sopaheluwakan, A. (2024). On the interannual variability of Indonesian monsoon rainfall: A literature review of the role of its external forcing. *Jurnal Meteorologi dan Geofisika, 24*(2), 115–127. https://doi.org/10.31172/jmg.v24i2.1049

Mulyanti, H., Istadi, & Gernowo, R. (2024). An insight from homogeneity testing of long-term rainfall datasets over East Java, Indonesia. *Journal of Emerging Science and Engineering, 2*(2), Article e23. https://doi.org/10.61435/jese.2024.e23

Mulyanti, H., Istadi, I., & Gernowo, R. (2023). Assessing vulnerability of agriculture to drought in East Java, Indonesia: Application of GIS and AHP. *Geoplanning, 10*(1), 55–72. https://doi.org/10.14710/GEOPLANNING.10.1.55-72

Ramadhani, F., Zarlis, M., & Suwilo, S. (2020). Improve BIRCH algorithm for big data clustering. *IOP Conference Series: Materials Science and Engineering, 725*, Article 012090. https://doi.org/10.1088/1757-899X/725/1/012090

Ruwangika, A. M., Perera, A., & Rathnayake, U. (2020). Comparison of statistical, graphical, and wavelet transform analyses for rainfall trends and patterns in Badulu Oya Catchment, Sri Lanka. *Complexity, 2020*, Article 7146593. https://doi.org/10.1155/2020/7146593

Sayyendra, A. P., Ariska, M., & Akhsan, H. (2025). Analysis of rainfall patterns in Papua using the empirical orthogonal function. Radiasi: *Jurnal Berkala Pendidikan Fisika, 18*(2), 93–102. https://doi.org/10.37729/radiasi.v18i2.6197

Weng, H., Ashok, K., Behera, S. K., Rao, S. A., & Yamagata, T. (2007). Impacts of recent El Niño Modoki on dry/wet conditions in the Pacific rim during boreal summer. *Climate Dynamics, 29*(2–3), 113–129. https://doi.org/10.1007/s00382-007-0234-0

Windari, E. H., Faqih, A., & Hermawan, E. (2012). El Niño Modoki dan pengaruhnya terhadap perilaku curah hujan monsunal di Indonesia. *Jurnal Meteorologi dan Geofisika, 13*(3), 149–160. https://doi.org/10.31172/jmg.v13i3.130

Wu, P. H., Lin, C. H., Chen, H., Wang, L., & Ho, C. R. (2025). Spatiotemporal variations and characteristics of the El Niño–Southern Oscillation phenomenon from 1950 to 2023. *Atmosphere, 16*(11), 1–13. https://doi.org/10.3390/atmos16111264

Zehri, S., Yulihastin, E., Marpaung, F., Adiputra, A., Mushoddik, Purwadani, N. N., & Gammamerdianti. (2025). Diverse impact of 2023 El Niño on weather patterns over the Indonesian Maritime Continent. *Journal of Southern Hemisphere Earth Systems Science, 75*(2), 1–14. https://doi.org/10.1071/ES25005

Zhang, T., Ramakrishnan, R., & Livny, M. (1996). BIRCH: An efficient data clustering method for very large databases. *Proceedings of the 1996 ACM SIGMOD International Conference on Management of Data*, 103–114.